

3. É. K. Kalinin, G. A. Dreitser, S. G. Zakirov, et al., Heat and Mass Transfer-VI. Materials of the VI All-Union Conference on Heat and Mass Transfer, Vol. 1, Part 1, Minsk (1980), pp. 100-111.
4. G. A. Dreitser, V. I. Gomon, and I. Z. Aronov, Prom. Teplotekh., 3, No 6, 36-42 (1981).
5. V. P. Isachenko, V. A. Osipova, and A. S. Sukomel, Heat Transfer, Moscow (1969).
6. Yu. N. Bololyubov, V. P. Borovikov, G. V. Grigor'ev, et al., Increase in the Efficiency of Heat Transfer in Power-Plant Equipment [in Russian], Leningrad (1981), pp. 174-179.
7. Yu. M. Brodov, Teploénergetika, No. 12, 36-40 (1982).

EVALUATING THE SPECTRUM OF DIMENSIONS OF VAPOR OCCLUSIONS  
BY THE ELECTRIC PROBING METHOD

E. P. Svistunov, V. P. Sevast'yanov, V. K. Shanin, UDC 531.733:532.529.5:621.1.013  
and V. M. Kryukov

This article examines aspects of the use of conductimetric sensor-probes to study the structure of steam-water flows.

One of the main parameters governing heat transfer and fluid dynamics in gas-liquid systems is the volume concentration of the lighter phase - the true volumetric gas or vapor content  $\varphi_V$ . The value of  $\varphi_V$  is measured empirically using various integral methods, such as from the reduction in the intensity of radioactive radiation or the change in the mass or relative electrical conductivity of a layer of the two-phase mixture.

The distribution of occlusions of the light phase in the liquid can be characterized by the notion of the local probabilistic gas content  $\varphi$ . By this, we mean the probability of finding the light phase at a given control point. The value of  $\varphi$  in a steady flow can be obtained by probing with a sensor having a sensitive element whose dimensions are considerably smaller than the dimensions of occlusions of the components of the mixture. Knowing the total time the sensitive element is in the light phase  $\Sigma\tau_i$  during the chosen exposure  $T$ , we can find the probabilistic gas content from the relation

$$\varphi = \frac{\Sigma\tau_i}{T}. \quad (1)$$

For a given velocity of vapor occlusions  $w$ , the total time over which the sensitive element passes through the bubble along the chosen streamline is determined by the chords of interaction. With a nominal spherical shape, the maximum length of interaction corresponds to the diameter. The actual spectrum of dimensions of the spherical or spheroidal occlusions unambiguously determines the probability density function of the duration of the above events  $\rho(\tau)$  [1]. If there is an equal probability that the bubbles of the actual dimensional spectrum will be distributed over the volume of the mixture, then data obtained by the integral method will agree with the values of  $\varphi_V$  calculated from the diagram of  $\varphi$  in the control section [2].

In practice, the validity of the integral and local methods of measuring gas content is often questionable in large volumes, in dense tube bundles, and in channels of complex geometry. In these cases, the agreement just noted rarely occurs, so the results of probing take on an independent value. This is particularly so in the study of the dispersion and structure of two-phase flows. The present investigation is devoted to evaluating the above-mentioned structural characteristics of flows in power-plant equipment at a pressure of 6.0-6.4 MPa.

---

Scientific-Research and Planning-Design Institute of Nuclear Power Engineering. Translated from Inzhenerno-Fizicheskii Zhurnal, Vol. 55, No. 5, pp. 794-800, November, 1988. Original article submitted May 18, 1987.

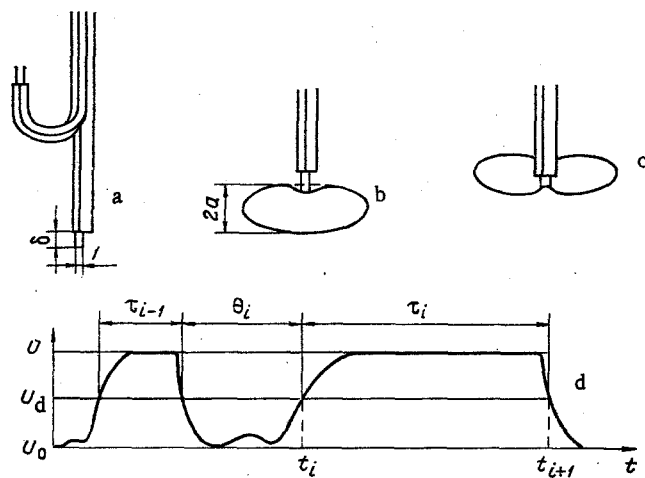


Fig. 1. Design of probe sensor (a), interaction of sensor with a vapor occlusion upon "piercing" (b) and exit (c) of the probe into the liquid phase, and oscillogram of the signal corresponding to the interaction process (d).

We determined  $\rho(\tau)$  using a method which has proven most successful in studies of two-phase systems and which involves the use of an electric probe to determine the time of passage of nonconducting vapor occlusions through a conductimetric cell. The measurement cell we used was nearly ideal with regard to minimizing its effect on the flow. It included an electrode formed by the end of a microconductor insulated over its entire length and an electrode whose dimensions were considerably greater than the linear dimensions of the bubbles [3]. This cell has practical value only for laboratory conditions, since its use is restricted to a limited range of gas contents for flow regimes in which the light phase is present in the liquid as individual occlusions. The usefulness of the cell is also limited by the absence of electrical-insulation materials for use in hot water. Improvements currently being made in the design of two-electrode sensors and measurement system are expanding the range in which it is possible to reliably evaluate gas content. These improvements will also alleviate the requirement for insulation and make it possible to conduct long-term experiments in a high-temperature steam-water medium [4].

In the general case, it is difficult to use a sensor with a measurement section in the form of two microelectrodes to study the structural parameters of two-phase mixtures within a broad range of  $\varphi$  (approximately from 0.05 to 0.95) because of the uncertainty in identifying the position of the electrodes in the liquid or vapor components of the flow from the change in the impedance of the measurement cell. When the sensor has been miniaturized to a certain point, the minimum electrical conduction between the microelectrodes is attributable to fluctuation of the thickness of the liquid film remaining on the surface of the structure at the moment the bubble passes under the probe. Here, the maximum conduction is attributable to the formation of drops from this film [4]. These extreme values are not stable and characterize the interaction of the flow and sensor at the stage after the bubble of the light phase is "pierced" by the microelectrodes. We can regard as relatively stable the intermediate value of electrical conductivity of the measurement section, corresponding to its position in the water. The method which is most convenient to use for commercial trials involves adjustment of the primary transducer. Here, the position of the probe in the light and heavy phases corresponds to stable maximum and minimum output values. Such a method is realized by using a transformer bridge with a grounded neutral conductor as the primary transducer [4], shielding the nonworking sections of the microelectrodes with metal jackets, and increasing the electrode spacing to 1 mm while using microelectrodes with a diameter of  $\sim 0.2$  mm (Fig. 1a). During the movement of the vapor occlusions, the residual film acts as a resistance for leakage currents between the microelectrodes and their shields. Under the operating conditions of the bridge, the film does not affect the indication of disruption of the electrical circuit of the sensor by the nonconducting bubble. Meanwhile, an increase in the electrode gap prevents the formation of drops on the measurement section at the moment the light phase passes through the probe.

When a spheroidal occlusion with a minor axis  $2a$  is "pierced," the equipment records the deformation of the shell of the occlusion and the reduction in the velocity  $w_1$  of the phase boundary over the base  $\delta$  of the measurement section (Fig. 1b). The subsequent entry of the microelectrodes into the liquid phase is characterized by their wetting by the liquid, which on the average increases the effective rate of motion  $w_2$  of the phase boundary along the electrodes (Fig. 1c). The output signal corresponding to this interaction is shown in Fig. 1d. The maximum value of the signal  $U$  is reached when the microelectrodes are in the vapor bubble, while the minimum value  $U_0$  is reached in the liquid. The time the measurement section is in the light phase  $\tau_i = t_{i+1} - t_i$  is measured with a chosen level of discrimination  $U_d$  with allowance for the effective values of the time constants corresponding to the rise of the signal from  $U_0$  to  $U$  and its decay from  $U$  to  $U_0$  [4].

Similar measurements were made by electric probing in [4, 5]. However, when the investigators evaluated the spectrum of the dimensions of vapor occlusions in the peripheral zone of the draft section of a bubbler with a diameter of  $\sim 2$  m [4], they did so within a limited range of vapor contents corresponding to the mean value of corrected vapor velocity. This made it impossible to make any kind of generalizations. In experiments conducted in [5] with vertical tube bundle, an equiprobable distribution of light-phase occlusions across the test section was precluded by the effect of the walls in conjunction with the fact that the probe was positioned in the central part of the inter-tube cell. Thus, the results obtained here could not be analyzed by the method proposed in [1]. If allowance is made for the geometric dimensions of the cross section of the nominal inter-tube cell, theoretical values of the bubble-sensor interaction length make it possible to estimate the transition from nucleate to plug flow of the ascending fluid. We conducted our measurements in a large volume. We also evaluated the possibility of analyzing the flow structure not only with values of  $\tau_i$ , but also with values of the time intervals between successive pulses  $\theta_i$  (Fig. 1d).

We measured the probability density functions  $\rho(t)$  and  $\rho(\theta)$  in the range of measurement of  $\varphi$  0.1-0.8. It was assumed that the functions obtained were distorted as a result of the independent interaction of the bubbles with each electrode (violation of the condition of pointedness of the probe) and deformation of the phase boundary in the interaction of the electrodes with the bubble [2]. The effect of the change in the shape of a surfacing bubble of fixed volume was neutralized by the choice of exposure (up to 100 sec). Special attention was given to the orientation of the probe relative to the direction of the flow, since the efficiency with which  $\varphi$  can be monitored decreases markedly in the case of the opposite orientation [2]. On the sections where reversal of the circulation was anticipated, we monitored the flow direction with sensors with a mutually perpendicular orientation (Fig. 1a). The determination of descending motion required analysis of the results, since the spectrum of dimensions of the bubbles entrained by the descending motion differed from the spectrum for the ascending flow. The velocity of the light phase  $w$ , with a uniform feed into the section, was evaluated from theoretical values of local velocity that were corrected for the evaporation surface  $w_{cr}$ :

$$w = w_{cr} / \varphi, \quad (2)$$

while the velocity in the case of a nonuniform feed was evaluated from the velocity of the vapor-liquid boundary through microelectrodes of known length  $\delta$ :

$$w = 0.5(w_1 + w_2). \quad (3)$$

The corresponding values of  $w_1$  and  $w_2$  were calculated with allowance for the rate of rise of the front of the signal  $|\Delta U / \Delta t|$  at the values of  $t_i$  and  $t_{i+1}$  (Fig. 1d):

$$w_{1,2} = \frac{\delta}{U - U_0} \left| \frac{\Delta U}{\Delta t} \right|. \quad (4)$$

The maximum length of sensor-bubble interaction for spheroidal bubbles is determined by the passage of the sensitive element along the minor axis of the spheroid  $2a$  (Fig. 1b). Measurement of the intervals  $\tau_i$  allowed us to use the values of  $w$  to calculate the interaction length  $\ell_i$  and construct the probability density function  $\rho(\ell)$  for the lengths of interaction between the sensor and bubbles corresponding to an actual spectrum of dimensions. Figure 2 shows a graphic interpretation of the subsequent analysis of measurements in accordance with the method described in [1]. By combining occlusions with minor axes from  $\ell_i$  to  $\ell_{i+1}$ , we

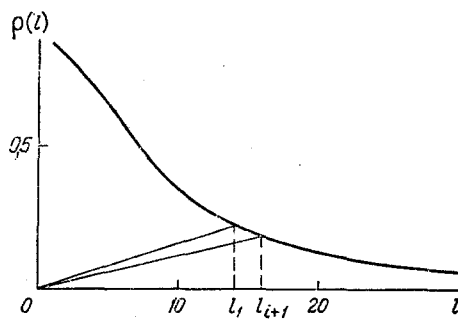


Fig. 2

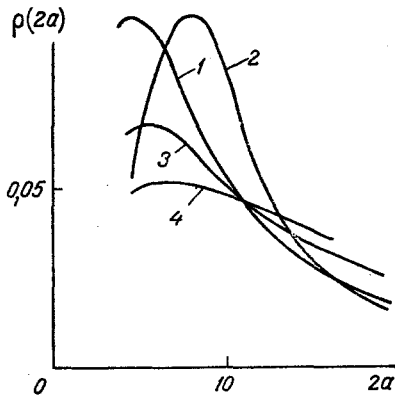


Fig. 3

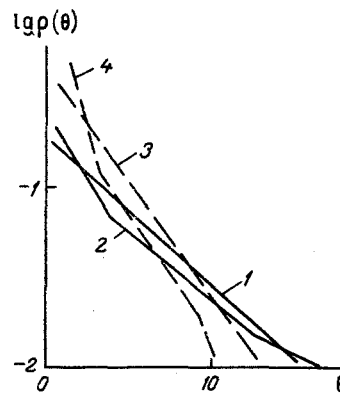


Fig. 4

Fig. 2. Probability density function of sensor-occlusion interaction paths in an actual flow.  $l$ , mm.

Fig. 3. Probability density function of the vapor occlusions regarding their contribution to the volumetric vapor content at a pressure of 6.4 MPa.  $2a$ , mm.

Fig. 4. Probability density function of intervals between vapor occlusions.  $\theta$ , msec.

find that the density distribution  $\rho(l)$  of interaction length for them is located between straight lines drawn from the coordinate origin to the point of intersection with the curve  $\rho(l)$  with the corresponding values of the abscissa  $l_i$  and  $l_{i+1}$ . Nearly tangential contact (minimum interaction length) of the sensor with a spherical or spheroidal bubble also corresponds to the minimum value of the density function [1]. We calculated  $\rho(2a)$  from the relation:

$$\rho(2a) = ka \left[ \rho(l) - l \frac{\Delta \rho(l)}{\Delta l} \right], \quad (5)$$

where  $k$  is the normalization constant.

After normalization with respect to unity, the density distributions obtained for the dimensions of the vapor occlusions in regard to the contribution toward true volumetric vapor content are as shown in Fig. 3.

According to the measurement data, for the bubbling of vapor through the liquid on the section corresponding to the dynamic two-phase layer (using the terminology in [6]), occlusions with a characteristic size  $2a$  from 4 to 8 mm (curves 1 and 2 in Fig. 3 for values of  $\varphi$  equal to 0.35 and 0.48, respectively) are most likely to contribute to the measured value of  $\varphi$ . The least likely values of  $2a$  correspond to stable bubbling in a large volume, while the most likely values correspond to the stabilization section. On this section, the light phase is discharged as a jet from the tube bundle or holes in the submerged perforated plate and enters the large volume. Accordingly, an equilibrium spectrum of dimensions is formed in this volume. On the transitional section from the dynamic two-phase layer to the vapor-

drop flow (in front of the nominal evaporation surface), the vapor occlusions undergo association - the curve  $\rho(2a)$  becomes simpler as the values of  $\varphi$  increase from 0.55 (curve 3) to 0.78 (curve 4). Here, the most probable value of  $2a$  remains almost unchanged. For most of the volume, the ordering of the structure of the mixture is determined by the distances between adjacent vapor occlusions. This distance can be evaluated from the probability density function  $\rho(\theta)$ , with allowance for the value of  $w$ . It was established experimentally that for the range of  $\varphi$  from 0.05 to 0.2 in air-water and steam-water flows, the structure of the flows - with a random distribution of light-phase occlusions over the volume of the mixture (nucleate flow regime) - is described by an exponential law conforming to the Poisson distribution

$$\rho(\theta) = \lambda \exp(-\lambda\theta), \quad (6)$$

where  $\lambda$  is determined by the ratio of the number of recorded vapor occlusions  $N$  to the corrected exposure of the record  $(1 - \varphi)T$ . Such a correction of the law of change in  $\rho(\theta)$  is needed to eliminate the effect of differences in the duration of each bubble-sensor interaction along the chosen streamline. Deviations occur from the law with an increase in vapor content. However, these deviations have a sufficiently convincing physical interpretation. For example, the results of calculation of  $\rho(\theta)$  from Eq. (6) are shown in Fig. 4 (curve 1) for a steam-water flow with a value of  $\varphi$  of  $\sim 0.48$ . Also shown is the empirical relation (curve 2). The values of  $T$  in the calculation were in milliseconds. The repeated discontinuities of the empirical curve  $\log \rho(\theta)$ , with sections that can be extrapolated as straight lines in the chosen coordinates, indicates the beginning of restructuring of the two-phase flow relative to the case of an equiprobable bubble distribution over the volume. The section  $\rho(\theta)$  for the minimum values of  $\theta$ , due to the passage of thin interlayers of liquid, begins with values of  $\lambda$  that are markedly greater than those predicted by calculation. This is evidence of a tendency toward association of the vapor occlusions. The slope-determining coefficient in the exponent is characterized not only by the law of distribution of the center-to-center distances between hypothetically associated bubbles, but also by the form of the vapor-liquid phase boundary. In the case of sufficiently dense packing of the light-phase spheroids, the form of the phase boundary determines the most probable interaction with the maximum length ( $\sim 2a$ ). If we allow for this, we can estimate the duration of the initial section  $2a/w$ . The change in the relation after the first discontinuity is due to ordering in the group between bubbles which did not enter the associated core. The subsequent transformation of the empirical curve is connected with the intervals between the passage of isolated groups of bubbles in the flow. The increase in vapor content in the transitional section from the vapor-water mixture to the vapor-drop flow smooths the transition between two adjacent sections of the experimental curve (coalescence of two groups of bubbles) and results in breakup of the liquid interlayers in the film that separate associated vapor occlusions. With an increase in the theoretical value of  $\lambda$ , this situation leads to an even greater difference from the experimental result in the region of minimum intervals  $\theta$ . Figure 4 also shows theoretical (curve 3) and experimental (curve 4) relations  $\log \rho(\theta)$  for a vapor content of 0.78. In laboratory tests involving flow visualization, the flow was identified as foamy on the basis of an increase in the experimental values of  $\lambda$  for the minimum intervals by a factor of 2.0-2.5 relative to the theoretical mean values. This increase, along with the change in the actual spectrum of dimensions of the vapor occlusions, can be used to estimate the transition from nucleate to foamy flow of a vapor-water mixture in a large volume.

#### NOTATION

$\varphi_v$ , true volumetric vapor content;  $\varphi$ , local vapor content;  $i$ , subscript to designate the serial number of an event;  $\tau$ , residence time of the probe in the vapor bubble;  $\theta$ , duration of interval between successive vapor occlusions;  $T$ , exposure;  $2a$ , minor axis of elliptical vapor occlusion;  $\rho$ , probability distribution function;  $\delta$ , length of microelectrodes of the probe;  $w_1$  and  $w_2$ , rate of movement of phase boundary past electrodes upon entry and exit of the probe from the vapor occlusion, respectively;  $w$ , velocity of vapor occlusion;  $w_{cr}$ , velocity of light phase corrected for the area of the evaporation surface;  $U$  and  $U_0$ , maximum and minimum amplitudes of signal at the output of the primary transducer (sensor);  $U_d$ , level of discrimination of the output-signal envelope;  $t$ , time;  $l$ , length of interaction of the sensor with a vapor occlusion;  $k$  normalization factor;  $N$ , number of recorded vapor occlusions;  $\lambda$ , frequency of passage of vapor occlusions;  $\delta$ , increment of a quantity;  $\Sigma$ , sum.

## LITERATURE CITED

1. R. A. Herringe and M. R. Davis, *J. Fluid Mech.*, **73**, Part 1, 97-123 (1976).
2. V. P. Sevast'yanov, B. P. Golubev, and E. P. Svistunov, *Teploénergetika*, No. 12, 58-60 (1984).
3. L. Z. Shenderov, A. G. Kvashnin, and V. V. Dil'man, *Inzh.-Fiz. Zh.*, **38**, No. 6, 1005-1010 (1980).
4. B. P. Golubev, S. N. Smirnov, Yu. M. Lukashov, and E. P. Svistunov, *Electrophysical Methods of Studying the Properties of Heat-Transfer Agents* [in Russian], Moscow (1985).
5. E. P. Svistunov, N. B. Éskin, V. P. Sevast'yanov, and A. S. Grigor'ev, *Teploénergetika*, No. 11, 40-43 (1984).
6. M. A. Styrikovich, O. I. Martynova, and Z. L. Miropol'skii, *Steam Generation Processes in Electric Power Plants* [in Russian], Moscow (1969).

MAXIMUM THICKNESS OF A TWO-PHASE LAYER DURING BOILING  
ON A FLAT HORIZONTAL SURFACE TURNED DOWNWARD

Yu. A. Kirichenko, K. V. Rusanov, and E. G. Tyurina

UDC 536.248.2.001.5

A study is made of the effect of the thermal load and pressure on the thickness of the two-phase layer in the boiling of water and nitrogen.

The boiling of liquid on a flat heating surface turned downward is characterized by low values of the critical thermal load and the heat-transfer coefficient in the sheet boiling regime [1]. A theory of heat transfer for such a heater orientation has yet to be developed; to construct such a theory, it will be necessary to have information on the dynamics of the vapor phase during boiling. Éskin, Kirichenko et al. [2] obtained data on the form and dimensions individual bubbles; it was found in particular that their thickness  $\delta$  may not exceed a certain limiting value  $\delta_{\text{lm}}$  associated with the capillary constant  $b$  and the contact angle  $\alpha$  (at  $\alpha \rightarrow 0^\circ$ ,  $\delta_{\text{lm}} \approx 2b$ ). In the nucleate boiling regime, growing and moving bubbles form a two-phase layer of the thickness  $\delta_{\text{tp}}$ . In sheet boiling, the thickness of the vapor film depends to a considerable extent on the heat-transfer rate. Data on the thickness of the two-phase layer or film is very valuable for constructing a model of the heat-transfer crisis during sheet boiling. However, the literature does not contain any such data.

The present study reports results of an investigation of the dependence of the maximum thickness of the two-phase layer  $\delta_{\text{tp}}$  on pressure, the type of liquid, and the heat flux  $q$  at different stages of boiling. Tests were conducted with boiling water (atmospheric pressure) and nitrogen (pressure from 0.02 to 0.9 MPa) in the saturated state. The method used to photograph the process was described in detail in [2]. We took 3-5 photographs for each value of  $q$ . We used pictures enlarged fourfold to determine the maximum thickness of the vapor phase, i.e., the maximum distance of this phase from the heating surface. We then found the arithmetic mean of  $\delta_{\text{tp}}$  from individual frames and a series of frames. We also determined the standard deviation, which turned out to be equal to 10-15%.

The error of determination of the maximum thickness by the simple method we employed was also no greater than 10% at acceptably low values of  $q$ .

For clarity, Fig. 1 compares the data on heat flux in fractions of its critical value  $q_{\text{cr1}}$  ( $q_{\text{cr1}} = 2.87 \cdot 10^5 \text{ W/m}^2$  for water and  $6.07 \cdot 10^4 \text{ W/m}^2$  for nitrogen). In the case of developed boiling ( $q/q_{\text{cr1}} \geq 0.1-0.2$ ), the value of  $\delta_{\text{tp}}$  is nearly independent of  $q$ . It can be seen from the figure that the thickness of the two-phase layer even decreases somewhat with the onset of the crisis ( $q/q_{\text{cr1}} = 1$ ). In the photographs, sheet boiling appears as a single

---

Physicotechnical Institute of Low Temperatures, Academy of Sciences of the Ukrainian SSR, Kharkov. Translated from *Inzhenerno-Fizicheskii Zhurnal*, Vol. 55, No. 5, pp. 800-803, November, 1988. Original article submitted July 7, 1987.